

A Long-Range, Fully-Integrated, Regulator-less CMOS Power Amplifier for Wireless Sensor Communications

William Wesson, Venumadhav Bhagavatula, Ka Wo Pang,

Soonkyun Shin, Pohan Yang and Jacques C. Rudell

Department of Electrical Engineering, University of Washington, Seattle, WA

Abstract—A CMOS PA system intended for long-distance sensor communication is presented. The PA utilizes a dynamic- V_{DD} and operates directly off of a super-capacitor energy-storage element, obviating the need for a voltage regulator. A power-combining PA impedance scaling approach has been implemented to eliminate energy loss from a high-current voltage regulator. The device integrates a 2-to-1 power combiner with a set of pre-drivers and an output stage. The PA monitors the output power, and digitally modulates the PA load impedance. The entire power control loop is integrated in a 90nm, 9-metal-layer TSMC process and delivers 24dBm of output power at 1.9GHz, making it suitable for sensor data communication over distances of several hundred meters. During a TX-burst, the PA V_{DD} varies from 2.5V to 1.4V, while the power control loop maintains constant output power with an accuracy of 1.6dB.

Keywords—CMOS PA, Impedance Modulation, Power Control Loop, Regulator-less Power Amplifier, Wireless Sensor Networks

I. INTRODUCTION

The evolution of small form-factor, single-chip wireless transceivers has enabled many new and previously unimaginable forms of connectivity. One such area which has benefited from low-cost miniature radios is the ability to not only acquire information from micro-sensors, but also transmit this data in real time over a wireless link. For the past decade, researchers have been exploring new circuit topologies, radio architectures, networking methods, and approaches to energy scavenging which allow autonomous operation of wireless transceivers for sensor data communication [1]. The very nature of sensor applications typically demands that a single device reside remotely, potentially for several years; thus, much research effort has been placed on minimizing the transmit energy on a per-bit basis. Collaborative mesh networks theoretically provide the most energy-per-bit efficient solution to transmit data over a given distance. However, numerous challenges limit the practical use of mesh networking including receiver wakeup time synchronization, network self-assembly in randomly deployed situations, and the challenge of coordination when a sensor node becomes mobile.

As an alternative, our work seeks to explore transceiver systems which enable long-distance sensor communication using conventional sources of renewable energy; in this case, solar cells. Sensor applications requiring low-spatial density or highly mobile situations would be enabled by a transceiver tailored for long-distance communication. Moreover, integration would enable programmability, possibly allowing future sensor nodes to “network scavenge,” further enhancing coverage area. The increased transmission distance would enable applications in areas of environmental monitoring, wildlife and object tracking, and homeland security [1], to name a few.

This paper addresses one of the most challenging transceiver components in the vision of long-distance, single-hop wireless sensor communication: the PA. In section II, the concept of a regulator-less, dynamic-impedance scaling PA is described. This is followed by section III, which gives a system and circuit description of the PA, the impedance scaling matching network, and the integrated power control loop. Finally, measured results and concluding comments are given in sections IV and V.

II. REGULATOR-LESS POWER AMPLIFIER

Although there are a number of challenges which must be addressed to realize small form-factor, autonomous, long-range sensor transceivers, one key issue is the realization of the transmitter and power amplifier. The presented PA is designed to operate with a super capacitor energy storage element, which supplies a voltage for the entire transceiver. During a TX burst, the super capacitor discharges and the supplied voltage will drop. Conventional wisdom suggests that a regulator should be used to maintain a constant supply voltage to the transceiver electronics. However, the implementation of this regulator, particularly for high-output power PA applications, can be challenging. While high-efficiency switching regulators can potentially boost the voltage as the capacitor discharges, the spurious signals introduced to the PA will corrupt the output spectrum. A Low Dropout Regulator (LDO) would reduce the likelihood of spurious emission, however this would be at the expensive of

degrading the overall transmitter efficiency, particularly at the beginning of the TX burst when the voltage drop across the LDO would be maximum. Therefore, the approach described in this paper attempts to eliminate the PA regulator. However, to maintain a constant output power during a TX burst, the output impedance must be dynamically varied as the super capacitor voltage begins to drop; the concept is illustrated in Fig. 1.

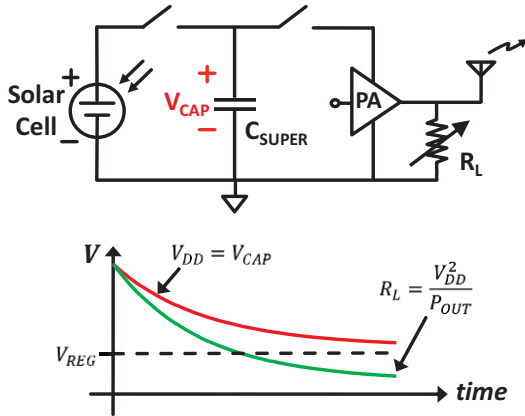


Fig. 1. Sensor PA concept illustrating the relationship between PA V_{DD} , PA output power, P_{OUT} , and PA load impedance R_L .

III. CIRCUIT DESIGN

The block diagram of the regulator-less, variable load impedance power amplifier is shown in Fig.2. The system is comprised of three major sections: a forward signal path consisting of an injection-locked LC-oscillator PA driver and a Class-E Power Amplifier, a tunable Impedance Transformation Network (ITN), and a feedback path operating as a power control loop.

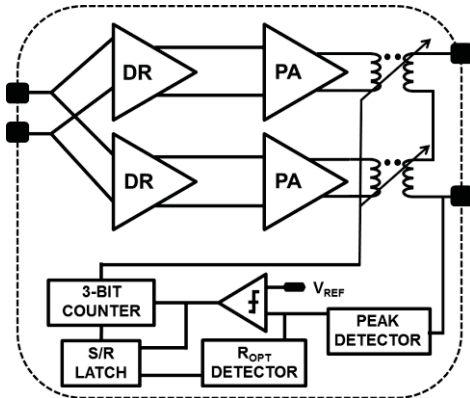


Fig. 2. Fully-integrated PA block-level diagram

A. Pre-Driver and PA : Signal Path

An external RF-signal is applied to the input of an injection-locked LC-oscillator (ILO) PA pre-driver stage,

shown in Fig.3(a). The ILO has a free-running frequency (ω_0) of 1.9GHz and a simulated lock range greater than 175MHz at all supply levels. The large gate capacitance of the PA switching device has been incorporated into the resonant tank of the oscillator. A pseudo-differential class-E switching PA with finite slab inductance drives the power combiner, as shown in Fig. 3(b). Compared to Class-E PAs with choke inductances, the slab inductor allows for complete integration of all passives loading the PA, and permits a higher load resistance for the same output power [2, 3]. To improve the reliability of the thin-oxide common source devices from large voltage swings, a thick-oxide cascode transistor is used [4].

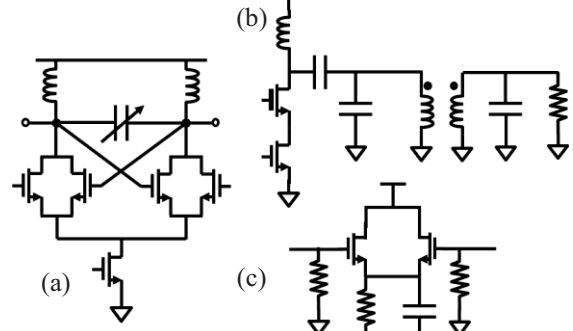


Fig. 3. Schematic diagrams of the a) ILO pre-driver, b) Class-E output stage and c) Class-C peak detector

B. Tunable Impedance Transformation Network (ITN)

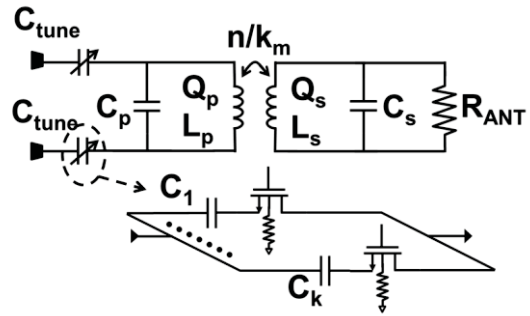


Fig.4 ITN fixed and variable impedance structures

A two stage ITN is implemented to convert the antenna impedance into an optimal load for the PA. A fixed impedance transformation of 1:8 has been achieved with a 2-to-1 series power combiner architecture, where each integrated transformer has a turns-ratio of 1:2. This fixed transformation converts the antenna impedance (R_{ANT}) to R_{TXF} , the minimum load resistance the PA requires in order to extract maximum output power (P_{OUT}) at minimum supply voltage. To maintain constant P_{OUT} at higher supply voltages, the load resistance is tuned using a variable series capacitance, C_{TUNE} , as shown in Fig. 4. For the sake of

clarity, a single transformer has been shown instead of the complete power combiner. Using a series-to-parallel conversion at ω_0 , an effective variable shunt resistance (R_P) is realized with a variable series capacitance, as seen in the following equations, where $Q=(\omega_0 RC_{TUNE})^{-1}$

$$R_P = (1 + Q^2)R_{TXF}; \quad C_P = \frac{Q^2}{1 + Q^2}C_{TUNE} \quad (1)$$

From (1), one observes that the effective shunt resistance and capacitance (R_P and C_P) loading the PA change by varying C_{TUNE} . Since the Class-E PA topology, by design, requires a large C_P for a high P_{OUT} , the variation in effective shunt capacitance due to variations in C_{TUNE} (~5% variation in C_P) results in negligible change of the ITN resonant frequency.

The series capacitor C_{TUNE} is realized with a 3-bit binary-weighted array. The associated switches require minimal loss and must handle the high voltages present at the PA output. Therefore, series resistors were placed on the gate and bulk terminals. The switch bulk resistors were created using a high-resistivity native substrate region in the area of the switch, as was done in [5].

C. Power Control Loop: Feedback Path

A Power Control Loop (PCL) provides feedback to automatically tune the ITN to a desired PA output power level, thus allowing a large V_{DD} variation during a TX burst. An external reference voltage sets the desired P_{OUT} and a trigger signal is used to initiate the control loop. A block diagram of the PCL is shown in Fig. 2.

An on-chip capacitive coupler sends an attenuated version of the output signal to a source follower Class-C peak detector circuit, shown in Fig. 3(c). This circuit provides a DC output voltage proportional to P_{OUT} . A comparator follows the peak detector and determines whether P_{OUT} is greater-than or less-than the desired value. A digital R_{OPT} detector signals if P_{OUT} peaks before the minimum load resistance is reached. The ITN switches are controlled by a 3-bit counter. During calibration, the 3-bit counter is reset and the PA begins incrementing from the lowest power state. The PCL cycles through all impedance states, with increasing power levels, until one of three conditions occurs: the desired output power is achieved, the minimum load impedance is achieved, or R_{OPT} is reached. The PCL then locks at and remains in this state, until it receives the next trigger signal.

IV. MEASUREMENT RESULTS

The fully-integrated PA is fabricated in a 90nm 9-metal TSMC CMOS process and occupies 1.92mm x 1.92mm including bond pads. On-wafer probing is performed on a

die assembled with test board using chip-on-board packaging. A die-photo is shown in Fig. 5.

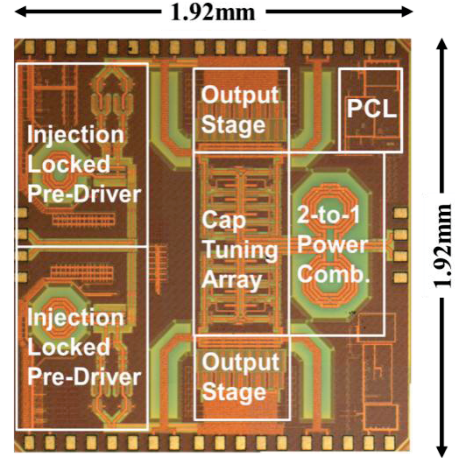


Fig.5. Chip Microphotograph

The output power (P_{OUT}) as a function of the ITN switch settings is shown in Fig. 6. For a fixed 1.5V supply (V_{DD}), P_{OUT} varies from 19.8 to 21.3dBm as the switches sweep through all possible settings, whereas for a 2.5V supply, the range is from 22.4 to 24dBm. From Fig. 6, one observes that P_{OUT} monotonically increases as the switch settings of the tuning network increase from 000 to 111.

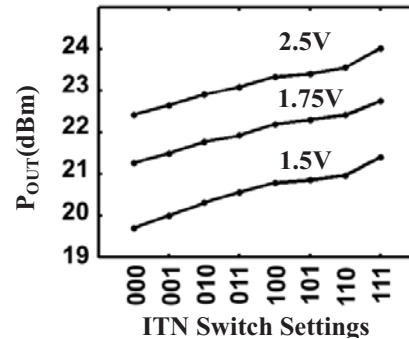


Fig. 6. P_{OUT} as a function of ITN Settings at different V_{DD}

Capacitor values in the tuning network were selected to achieve a power-control granularity of 0.2 dB at the expense of a power-range of 1.5-1.7dB. Fig. 7 displays a constant PA output power of +21.6dBm within ± 0.2 dB across a supply-range of 0.35V (1.55V to 1.9V) and within ± 0.8 dB across a range of 1.1V (1.4 to 2.5V). The peak efficiency of the PA is 10.2% and varies by less than 2% over the full V_{DD} range. The PA resulted in a measured efficiency substantially lower than originally designed and simulated. The need for high-voltage CMOS switches requires a large spacing between elements in the capacitor array, thus requiring long interconnects in the PA ITN. The additional power/efficiency loss is attributed to inaccurate modeling of these long traces. At present, we are investigating methods to eliminate the need for high-

voltage CMOS switches while still achieving a high output power solution.

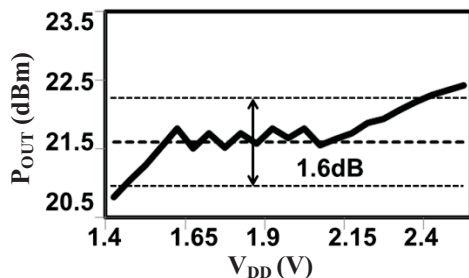


Fig.7. Constant output power vs. supply voltage

PCL functionality is verified with the help of an on-board power-detector. The output voltage of the power-detector is proportional (in dB scale) to P_{OUT} . The transient response of the power-detector in response to an externally calibrated trigger is captured in Fig. 9. At time T_1 , the loop initiates from the low-power state and P_{OUT} sequentially increases until time T_2 , where P_{OUT} locks to the desired power specified by the external reference. This is one of the first demonstrations of an integrated power control loop achieving regulator-less constant output power in a PA design.

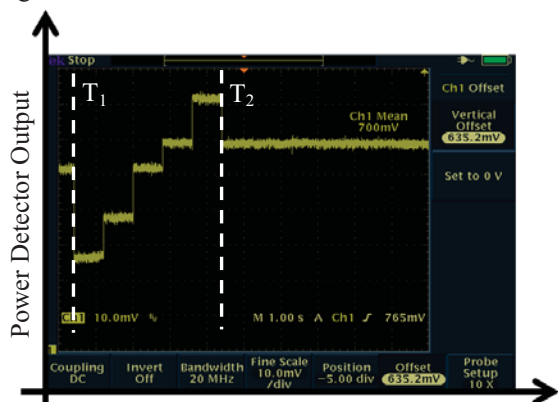


Fig. 9. Constant output power vs. supply voltage

Table I gives a performance summary and comparison to other published results. While the concept of a PA for wide-area sensor networks is new, there has been considerable interest in tunable output matching networks to optimize PA efficiency under large back-off conditions. [6] and [7] report off-chip varactor and switch-capacitor based matching networks respectively. [7] also reports an off-chip PCL. This work achieves a higher degree of PCL integration for load modulation than prior-art.

V. CONCLUSION

A long-range, regulator-less power amplifier with dynamic load impedance tuning has been presented. By

removing the voltage regulator in a wireless sensor PA, the overall transmitter efficiency can be increased, directly translating to longer transmission periods. A new transformer-based impedance tuning approach is given, showing promise towards dynamically varying the PA load impedance to accommodate wide variations in the supplied voltage. Future work could extend these concepts towards realizing an effective integrated load-pull PA to improve efficiency and linearity for variations in antenna impedance.

TABLE I
COMPARISON OF PUBLISHED WORKS

	[6]	[7]	This Work
Tech	LDMOS	130nm CMOS	90nm CMOS
Matching Network	Off-Chip Inductor	Off-Chip Inductor	On-Chip Txfmr
Tuning Method	Abrupt Junction Varactor	Off-Chip Switched Capacitor	On-Chip Switched Capacitor
Control Loop	Not Present	Off-Chip	On-Chip
Power Output	39dBm @ 1GHz	19dBm @ 0.8GHz	21.5dBm @ 1.9GHz
Key Results	10% η increase @ 10dB back-off	20% η reduction @ 6dB back-off	< 1.6dB power variation @ 1.5V to 2.5V

REFERENCES

- [1] Bhagavatula V., et al. "Green Monitoring using a Wide Area Radio Network for Sensor (WARNS) Communication," in *Proc. of IGCC*, 2011.
- [2] Grebennikov, A., *RF and Microwave Power Amplifier Design*. New York: McGraw-Hill Professional Engg, 2005.
- [3] Walling, J. S., et al., "A Class-E PA with Pulse-Width and Pulse-Position Modulation in 65nm CMOS," *IEEE JSSC*, Vol. 44, No. 6, pp. 1668-1678, June 2009.
- [4] Mazzanti, A. et al., "Analysis of Reliability and Power Efficiency in Cascode Class-E PAs," *IEEE JSSC*, Vol. 41, No. 5, pp. 1222-1229, May 2006.
- [5] Kidwai, A. A., et al., "A Fully Integrated Ultra-Low Insertion Loss T/R Switch for 802.11b/g/n Application in 90nm CMOS Process," *IEEE JSSC*, Vol.42, No.5, Pp. 1352-1360, May 2009.
- [6] H.M.Nemati et al. "Design of Varactor-Based Tunable Matching Networks for Dynamic Load Modulation of High Power Amplifiers", in *IEEE MTT*, Vol.57, No.5, May 2009
- [7] N.Singhal et al. "A 19dBm 0.13um CMOS Parallel Class-E Switching PA with Minimal Efficiency Degradation under 6dB Back-off" in *IEEE RFIC Symposium Dig. of Papers*, Pg.553-556, June 2011.